

RESEARCH ARTICLE

The Investigation of Structural, Optical and Thermal Properties of Nickel Doped CeO₂ Integrated PVC Nanocomposite

Rishum Khan¹ | Muhammad Tariq Qamar¹ | Hina Abid¹ | Irfan Haider² | Ammar Zidan³ | Ali Bahadur^{4,5} | Shahid Iqbal⁶  | Sajid Mahmood^{6,7} | Mohammed T. Alotaibi⁸ | Toheed Akhter⁹

¹Department of Chemistry, Forman Christian College (A Chartered University), Lahore, Pakistan | ²National Centre for Physics, Quaid-e-Azam University, Islamabad, Pakistan | ³Biomedical Engineering Department, College of Engineering and Technologies, Al-Mustaqbal University, Babylon, Iraq | ⁴Department of Chemistry, College of Science, Mathematics, and Technology, Nanomaterials Research Center, Wenzhou-Kean University, Wenzhou, China | ⁵Dorothy and George Hennings College of Science, Mathematics and Technology, Kean University, Union, New Jersey, USA | ⁶Nottingham Ningbo China Beacons of Excellence Research and Innovation Institute, University of Nottingham Ningbo China, Ningbo, China | ⁷Functional Materials Group, Gulf University for Science and Technology, Mishref, Kuwait | ⁸Department of Chemistry, Turabah University College, Taif University, Taif, Saudi Arabia | ⁹Department of Chemical and Biological Engineering, Gachon University, Seongnam, Republic of Korea

Correspondence: Sajid Mahmood (sajidmahmood1987@yahoo.com) | Shahid Iqbal (shahid iqbal@hzu.edu.cn)

Received: 13 June 2024 | **Revised:** 31 August 2024 | **Accepted:** 22 September 2024

Review Editor: Mingying Yang

Funding: The authors extend their appreciation to Taif University, Saudi Arabia for supporting this work through project number (TU-DSPP-2024-180).

Keywords: Ni-doped CeO₂ nanofiller | PVC NCs | SEM | TGA/DSC | XRD

ABSTRACT

PVC nanocomposite (NC) films with cubic CeO₂ and Ni-doped CeO₂ (NDC) have been prepared using a conventional solution-casting technique. The prepared films were characterized with FT-IR spectrometer, X-ray diffraction (XRD), and scanning electron microscopy (SEM). The optical and thermal properties of the films were evaluated using a UV-visible spectrophotometer and TGA/DSC. The optical study revealed a decrease in optical band gap energies (4.19 to 4.06 eV) whereas the increase in other optical constraints such as optical conductivity, Urbach energy, dispersion energy, refractive index, and dielectric constant of PVC NCs than pristine PVC was observed. The XRD patterns showed the presence of cubic crystalline NDC with a relatively narrower principal diffraction peak in the PVC matrix and the nonexistence of unexpected vibrational peaks in the FTIR spectra of PVC NCs confirmed the successful incorporation of nanostructured CeO₂ and NDC into PVC. Thermogravimetric analysis showed the higher thermal stability of NDC/PVC NC than PVC whereas differential scanning calorimetry declared no significant change in the glass transition temperature (T_g) of the NCs. Moreover, a good dispersion of Ni-doped CeO₂ nanofiller was noticed in scanning electron micrographs.

1 | Introduction

Polymer NCs are one of the leading materials due to their significant contribution in various modern-day disciplines such as environment, energy, and health care (Darwish, Mostafa, and Al-Harbi 2022; Zhang, Khorshidi et al. 2023; Zhang,

Huang et al. 2023). The upsurge performance of these materials is mostly attributed to the resultant properties that both polymer matrix and nanoscale reinforcement produce (Asture et al. 2023; Mansour et al. 2020). Nanoparticles as nanofillers have rapidly gained attention because of the versatility they bring to the materials' performance, especially by improving

Summary

- Using the solution casting process, PVC nanocomposite films containing CeO₂ and Ni-doped CeO₂ were successfully created.
- Additionally, scanning electron micrographs showed an excellent dispersion of Ni-doped CeO₂ nanofiller.
- The optical study showed that adding NDC to PVC caused its band gap energy to drop from 4.19 to 4.06 eV.
- A further indication that nanofillers had been added to the PVC matrix was the rise in Urbach energy.
- Although there was only a small difference in T_g, thermal studies showed that NCs had greater T₁₀ and T₅₀ values than pure PVC.

optical, structural, electrical, mechanical, and thermal properties, once incorporated into the polymer matrix (Romero-Fierro et al. 2022; Tamayo-Vegas et al. 2022). Al-Dhabi et al. tuned the dielectric, electrical, and optical properties of the polyethylene oxide/carboxymethyl cellulose blend by adding ZnO/GO as a nanofiller (Al-Harbi et al. 2023). Rahman et al. improved the optical, electrical, and mechanical properties of the polyester matrix by reinforcing with TiO₂, Fe₂O₃, and NiFe₂O₄ nanoparticles (Rahman et al. 2019). Safdari and his coworkers investigated the effect of Bi₂O₃ nanofiller on the sensing response of polycarbonate (Safdari et al. 2022). Recently, researchers explored the variation in optical, thermal, and structural properties of polyvinyl chloride/polyvinyl propylene blend with the addition of Er₂O₃ nanofiller for optoelectronic applications (Alshammari, Alshammari, Ibrahim et al. 2023).

PVC matrix NCs have attained substantial consideration in optoelectronic systems due to superior physical characteristics and tunable optical properties of PVC such as refractive index, transmittance, bandgap energy, fluorescence, optical oscillator strength, and optical susceptibility (Alshammari, Alshammari, Ibrahim et al. 2023; Hu et al. 2020; Taha and Azab 2019). Literature reveals that the optical properties of PVC can be tailored by introducing nanofillers in the PVC matrix to extend its scope in optical, electronic, and photonic systems (Taha and Azab 2019; Hashmi et al. 2022; Ebnalwaled and Thabet 2016). For example, Abouhaswa et al. reported an increase in PVC absorption with increasing CuO nanofiller content whereas the decrease in bandgap energy of PVC matrix nanocomposite (NC) was noticed (Abouhaswa and Taha 2020). Deshmukh et al. used different weight percentages of graphene oxide nanofiller to improve the properties of PVC (Deshmukh, Khatake, and Joshi 2013). El Sayed et al. explored the optical and dielectric properties of PVC/CdO NC films. They observed a decrease in bandgap energy from 5.07 to 4.89 eV with increasing nanofiller content whereas an increasing trend was reported for refractive index (El Sayed et al. 2014). Taha et al. explored the effect of SnO₂ nanofillers on the optical, structural, and thermal properties of PVC, and they concluded that the decrease in bandgap energy is mainly attributed to the Sn defects within the bands. Moreover, they also reported an increase in light absorption and refractive index of PVC NCs as compared to pure PVC (Taha, Ismail, and

Elhawary 2018). Moreover, TiO₂, ZnO, ZrO₂, CdS, and SiO₂ were also used as nanofillers to enhance the optical, structural, and mechanical properties of PVC (Abdel-Baset, Elzayat, and Mahrous 2016; Abdel-Gawad et al. 2017; Mallakpour and Darvishzadeh 2018; Patidar and Saxena 2013; Mallakpour and Shafiee 2017). Despite all these developments, it is still extremely desirable to investigate nanofillers about 3d-transition metal-modified rare-earth oxide to improve the features of PVC polymer.

In this context, CeO₂ as a nanofiller for polymers has been preferred due to its excellent physicochemical properties, structure compatibility, and higher UV absorption in comparison to conventional nanofillers such as TiO₂ and ZnO (Hu et al. 2020; Mishra and Mukhopadhyay 2021). For instance, James et al. used three different strategies to enhance the refractive index of polystyrene by adding CeO₂ nanoparticles for better utilization of polystyrene/CeO₂ NCs in photonics industries (James et al. 2019). In situ polymerization was used by Kumar et al. to create and characterize the polyaniline/CeO₂ NC. They reported the successful insertion of cubic CeO₂ nanoparticles in a polyaniline matrix with improved properties (Kumar, Selvarajan, and Muthuraj 2012). Hemalatha et al. investigated the optical properties of PVA by varying the amount of CeO₂ nanofiller content from 2.5 to 25wt%, and they reported homogeneous dispersion of CeO₂ content in the polymer which ultimately led to PVA NCs with excellent optical properties (Hemalatha and Rukmani 2016). The above-mentioned studies revealed that 3d-transition metal-doped CeO₂ nanofillers could be excellent alternatives to improve the various properties of PVC.

In this study, an effort has been made to explore the optical and physical properties of PVC NC films, prepared with our previously synthesized nickel-doped CeO₂ and pristine CeO₂ nanofillers through a solution-casting approach. The prepared films were further characterized using UV-visible spectrophotometer, XRD, FTIR, SEM, and TGA/DSC for evaluation of the optical, structural, morphological, and thermal properties of PVC NC films.

2 | Experimental

PVC (*K*-value 68–65, Macklin, China) was mixed with nickel-doped CeO₂ nanofillers to prepare PVC NC films by a solution-casting method (Taha and Azab 2019). Our previously reported Ni-doped CeO₂ (NDC) and pristine CeO₂ powders were used as nanofillers in this study (Qamar et al. 2023). In a typical preparation of PVC matrix NC film, 0.5g PVC was dissolved completely in 50 mL tetrahydrofuran (THF) at room temperature to form a clear solution. Then, 5 mg NDC powder was dispersed ultrasonically in above mentioned PVC solution for 1 h to make a homogeneous dispersion. The obtained dispersion was finally poured into a glass petri dish and dried in an oven at 50°C for 48 h to get a PVC NC film. The obtained film was peeled off from the petri dish and denoted as NDC/PVC. A similar procedure was adopted to prepare PVC film with pristine CeO₂ powder and the obtained NC film was marked CeO₂/PVC. Moreover, pure PVC film was also prepared under similar conditions for comparison with

NC films. The thickness (0.48 mm) of the films was measured by screw gauge.

XRD patterns of films were recorded from 5° to 80° with 0.02° step size by X-ray powder diffractometer (Rigaku D-MAX/IIA, Japan) having Cu K α radiation. FT-IR spectra were attained on a Bruker Alpha II FTIR spectrometer. The SDT Q600 TGA/DSC analyzer from TA Instruments was used to perform TGA/DSC studies in a N₂ atmosphere at a heating rate of 20°C/min from 0°C to 600°C. A scanning electron microscope (SEM, S-3700N, Hitachi Hi-Technologies Corporation, Japan) was used to assess the surface morphology of the films. Moreover, a UV-visible spectrophotometer (UV-1800, Shimadzu, Japan) was used to record the absorption spectra of the films.

3 | Results and Discussion

The optical absorption and transmittance (%) spectra of PVC and its composites are presented in Figure 1. In absorption spectra, an increase in absorption is noticed with the addition of CeO₂ and NDC. The enhanced absorbance of NCs may be attributed to the increase in surface area of the NC due to the addition of nanofillers in the PVC matrix (Kassem et al. 2023). Moreover, the incorporation of NDC has yielded a new broad band ranging from 310 to 412nm which is absent in the absorption response of CeO₂/PVC NC. The appearance of this broadband can be attributed to the formation of the complex between PVC and NDC (Kassem et al. 2023). Moreover, the absorption band from 254 to 294nm and high absorption peaks below 240nm are due to π - π^* transitions and C-Cl bond in PVC (Taha and Azab 2019). The Inset figure demonstrates the suppression of the optical transmittance of PVC upon the incorporation of nanofillers. For instance, the transmittance of PVC at 500nm is reduced from ~97% to ~57% due to the addition of CeO₂ in the PVC matrix which is further reduced to ~34% while adding only NDC in PVC.

Figure 2 demonstrates the evaluation of optical band gap energy (E_{opt}) for both direct and indirect allowed transitions,

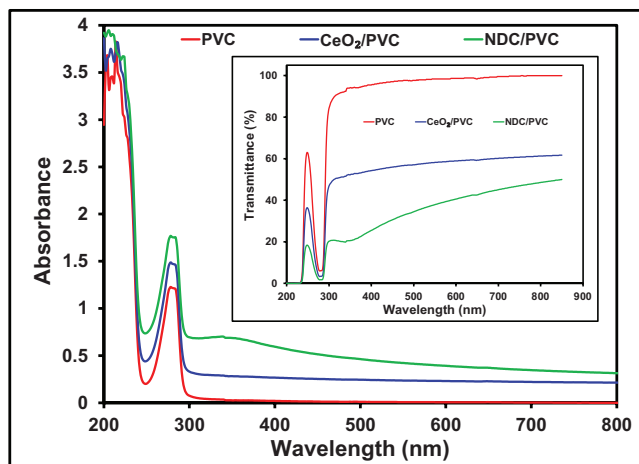


FIGURE 1 | The comparison of absorption spectra of PVC and its composites, whereas inset is the transmittance (%) spectra of the materials.

respectively in the materials. The following Equations (1) and (2) are used to estimate the band gap energies (Alshammari, Alshammari, Alshammari et al. 2023);

$$\alpha hv = k(hv - E_{direct})^{0.5} \quad (1)$$

$$\alpha hv = B(hv - E_{indirect})^2 \quad (2)$$

Where B is a constant. The E_{direct} and $E_{indirect}$ in eV are estimated while extrapolating the linear portion of curves obtained from $(\alpha hv)^2$ versus hv and $(\alpha hv)^{0.5}$ versus hv to zero absorption as shown in Figure 2a,b, respectively. The addition of CeO₂ and NDC nanofillers has reduced both direct and indirect band gap energies of the PVC which are summarized in Table 1. Furthermore, relatively greater linearity in $(\alpha hv)^{0.5}$ versus hv curve as compared to the curve obtained in $(\alpha hv)^2$ versus hv depicts mainly an indirect nature of transitions in PVC NCs from valance band to the conduction band (CB). This decrease in band gap energy can be attributed to the possible formation of new localized electronic states due to NDC between the valance band (VB) and CB of the PVC. These states can contribute to low energy transitions which ultimately lead to the lowering of effective band gap of the NDC/PVC NC (El-Naggar et al. 2023). In addition, the higher conductivity introduced in PVC matrix due

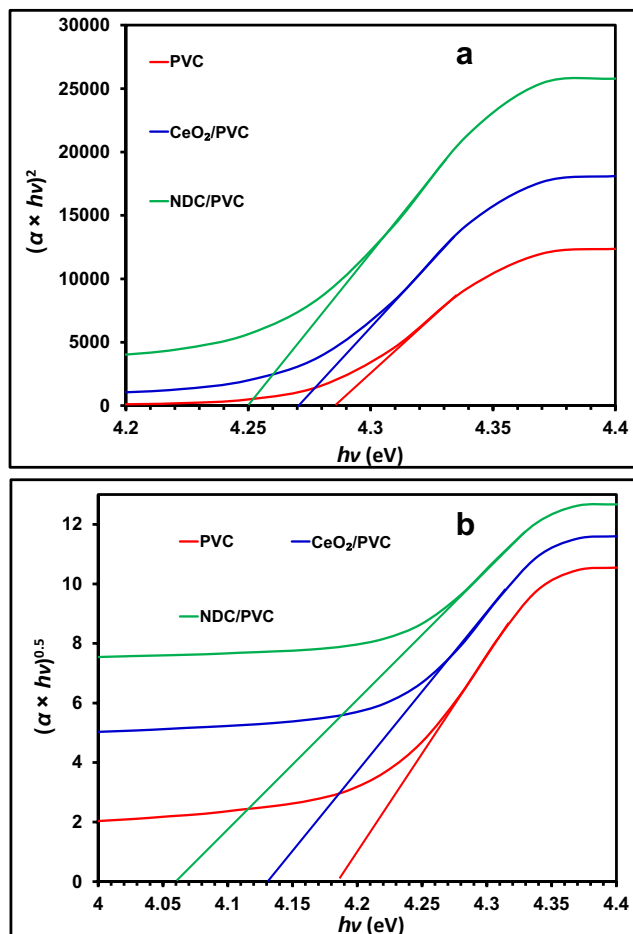


FIGURE 2 | (a) direct and (b) indirect band gap evaluation of pure PVC and its NCs.

TABLE 1 | Optical parameters of pure PVC and its NCs with CeO₂ and Ni-doped CeO₂ (NDC).

Optical Parameter		PVC	CeO ₂ /PVC	NDC/PVC
λ_{max} (nm)		290	290	290
Optical bandgap energy “ E_{opt} ”	Direct (eV)	4.29	4.27	4.25
	Indirect (eV)	4.19	4.13	4.06
Urbach energy “ E_u ” (meV)		61	108	173
Average excitation energy “ E_o ” (eV)		4.02	6.67	4.18
Dispersion energy “ E_d ” (eV)		0.94	23.06	22.95
Static refractive index “ n_o ”		1.11	2.11	2.54
Static dielectric constant “ ϵ_s ”		1.23	4.45	6.48
Moments of optical spectrum	M_{-1}	0.23	3.46	5.48
	M_{-3} (eV ⁻²)	0.01	0.08	0.31
Linear optical susceptibility “ $\chi^{(1)}$ ”		0.02	0.28	0.44
Nonlinear optical susceptibility “ $\chi^{(3)}$ ” (e.s.u)		2.05×10^{-17}	9.74×10^{-13}	6.16×10^{-12}
Nonlinear refractive index “ n_2 ” (e.s.u)		6.96×10^{-16}	1.74×10^{-11}	9.12×10^{-11}
High-frequency dielectric constant “ ϵ_∞ ”		2.07	6.34	22.27
Long-wavelength refractive index “ n_∞ ”		1.43	2.51	4.72

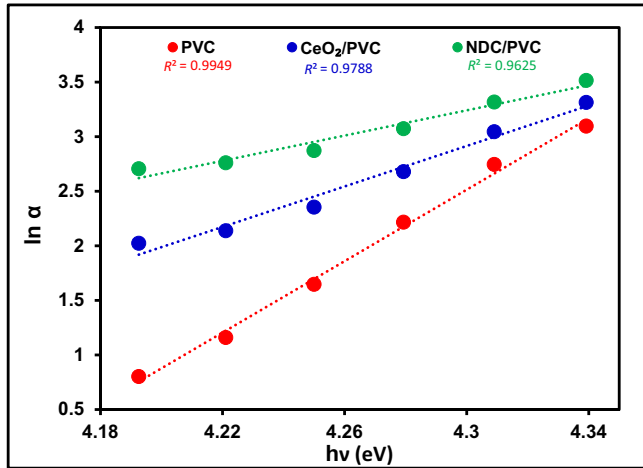


FIGURE 3 | $\ln \alpha$ versus $h\nu$ for the determination of Urbach energy of pure PVC and its NCs.

to NDC in comparison to CeO₂ can also be another reason for bandgap reduction. To estimate the disorder in films due to the possible formation of localized states within the forbidden band gap, the Urbach energy is calculated using Equation (4) (Taha and Azab 2019; Kassem et al. 2023);

$$\alpha = \alpha_o \times \exp(h\nu/E_U) \quad (3)$$

$$\ln(\alpha) = \ln(\alpha_o) + \frac{1}{E_U}(h\nu) \quad (4)$$

The Urbach energy (E_U) is estimated by calculating the reciprocal of slope ($\frac{1}{E_U}$) obtained from the curves between $\ln(\alpha)$ and $h\nu$ as shown in Figure 3. The estimated E_U values (meV) are provided in Table 1, which reveals an increase in imperfections or disorder

in the PVC matrix due to the addition of nanofillers. These imperfections usually occur due to the formation of transition states between the bandgap of PVC upon the addition of nanofiller in PVC matrix while distorting the structure of PVC. This distortion further broadens the Urbach tail and hence the Urbach energy with increasing density of the states (Taha and Azab 2019; Kassem et al. 2023).

The effect of nanofillers on the traveling of light in the PVC matrix is assessed by calculating the refractive index (n) of films using Equation (5). Moreover, the change in “ n ” of the samples with varying wavelengths from 400 to 850 nm is presented in Figure 4.

$$\text{Refractive Index } (n) = \left(\frac{1+R}{1-R} \right) + \left(\frac{4R}{(1-R)^2} - k^2 \right)^{0.5} \quad (5)$$

Where,

$$\text{Extinction coefficient } (k) = \frac{\alpha\lambda}{4\pi} \quad (6)$$

The refractive index of PVC NCs is observed significantly higher as compared to pure PVC matrix. The refractive index of PVC is in agreement with the literature however the existence of higher “ n ” values due to the addition of nanofiller is also evident in the literature (Taha and Azab 2019). These high refractive indices may be attributed to the higher packing density of the NC due to the incorporation of nanofiller in the PVC matrix which ultimately leads to the slowing of light traveling. Moreover, the strength of optical transitions between the bands (E_d) that is, dispersion energy and the average energy required for these excitations (E_o) that is, effective oscillator energy are determined from the slope and intercept in Figure 5 using Equation (7).

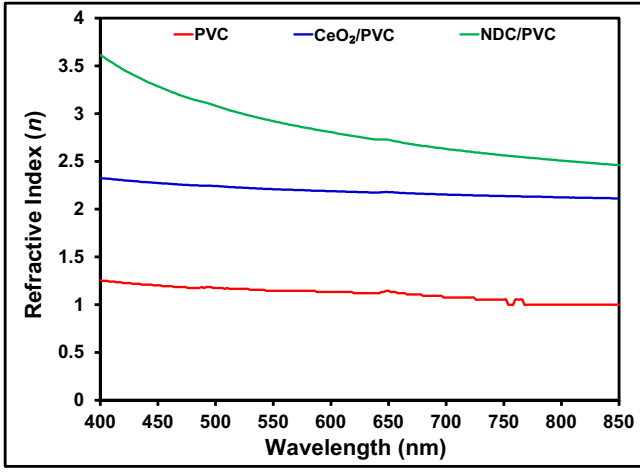


FIGURE 4 | The comparison of refractive index (n) of pure PVC and its NCs.

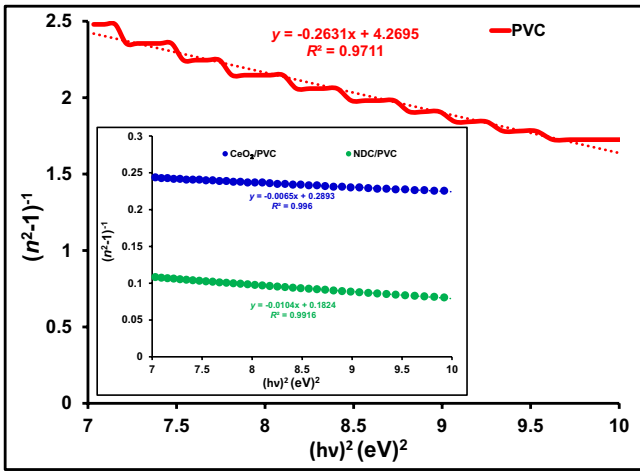


FIGURE 5 | $(n^2-1)^{-1}$ versus $(hv)^2$ plots for pure PVC and its NCs.

Moreover, static refractive index (n_o), static dielectric constant (ϵ_s), and optical oscillator strengths (f) are calculated using Equations (8)–(10).

$$\frac{1}{n^2 - 1} = \left(\frac{E_o}{E_d} \right) - \left(\frac{1}{E_o E_d} \right) (hv)^2 \quad (7)$$

$$n_o = \left(1 + \frac{E_d}{E_o} \right)^{0.5} \quad (8)$$

$$\epsilon_s = n_o^2 \quad (9)$$

$$f = E_o \times E_d \quad (10)$$

The calculated E_o , E_d , n_o , and f values are summarized in Table 1, which have been increased with the addition of nanofiller into the PVC matrix as compared to pure PVC matrix. The dispersion energy describes the energy associated with the interaction of nanofiller with PVC and their distribution within the PVC matrix. The lower dispersion energy corresponds to an easy dispersion of nanofillers within the matrix and good compatibility of both components. Table 1, shows a relatively greater compatibility and good dispersion of NDC as compared to pure

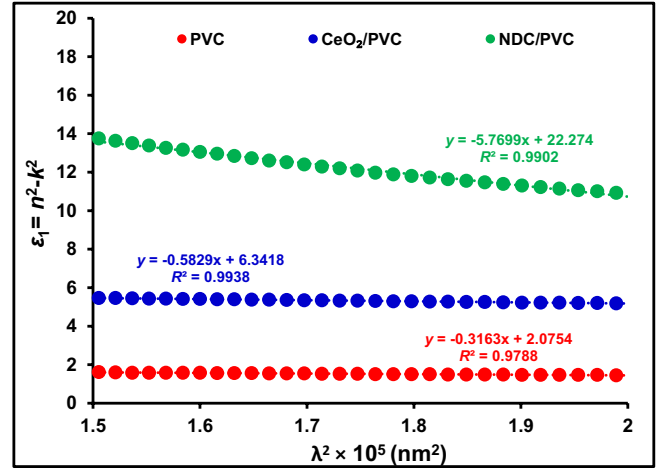


FIGURE 6 | The linear portion of real part of dielectric constant (ϵ_1) versus λ^2 plots for pure PVC and its NCs.

CeO₂ in PVC matrix which can be attributed to its lower size and greater surface area. Moreover, other optical parameters such as moments of the optical spectrum (M_{-1} and M_{-3}), linear and nonlinear optical susceptibilities (χ_1 and χ_3), and nonlinear refractive index (n_2) are tabulated in Table 1 which are calculated using the authentic mathematical equations provided in the literature (Taha and Azab 2019).

The increase in the real part of the dielectric constant (ϵ_1) is noticed with the addition of nanofillers in the PVC matrix as shown in Figure 6. Moreover, the high-frequency dielectric constant (ϵ_∞) is calculated using the following Equation (11);

$$\epsilon_1 = n^2 - k^2 = \epsilon_\infty - \left(\frac{e^4}{4\pi^2 c^2 \epsilon_o} \right) \left(\frac{N}{m^*} \right) \lambda^2 \quad (11)$$

ϵ_∞ is estimated from the intercept of ϵ_1 versus λ^2 plot as shown in Figure 6. Furthermore, ϵ_∞ is used to estimate long-wavelength refractive index (n_∞) while using $n_\infty = \sqrt{\epsilon_\infty}$.

Another important optical parameter that is, optical conductivity (σ_{opt}) is calculated using Equation (12) as shown in Figure 7. Optical conductivity helps to understand the movement of charge carriers while varying the electric field of incident electromagnetic waves.

$$\sigma_{opt} = \frac{n\alpha c}{4\pi} \quad (12)$$

The increase in optical conductivity of the PVC matrix with the addition of CeO₂ and NDC confirms the formation of new states within the bandgap which consequently leads to a reduction in bandgap energy of the NCs as compared to pure PVC matrix. Moreover, all calculated optical parameters are summarized in Table 1.

The comparison of XRD patterns of PVC and its NCs are presented in Figure 8. The appearance of diffraction planes at (2θ) 28.17°, 32.70°, 47.03°, 55.83°, 58.57°, 67.98°, 76.06°, and 78.42° in NCs shows the presence of cubic phase (JCPDS 34–0394) of CeO₂. However, the existence of similar diffraction planes with slightly changed 2θ values indicates the presence of NDC in

the PVC matrix. XRD analysis (Figure 8) also reveals that the peak broadening in cubic CeO_2 and NDC nanofillers has been decreased due to the presence of PVC as compared to their peak broadening shown in our previous finding (Qamar et al. 2023). Previously, 9.76 and 8.28 nm average crystallite sizes were noticed for pure CeO_2 and NDC, respectively (Qamar et al. 2023). However, these sizes were increased to 42.69 nm for CeO_2 and 33.16 nm for NDC in the presence of PVC. Moreover, it is also noticed that the cubic crystal structure of the nanofillers has not been changed inside the PVC matrix which indicates the successful incorporation of nanofillers in the PVC matrix. Moreover, the morphology of the PVC and its NCs are compared

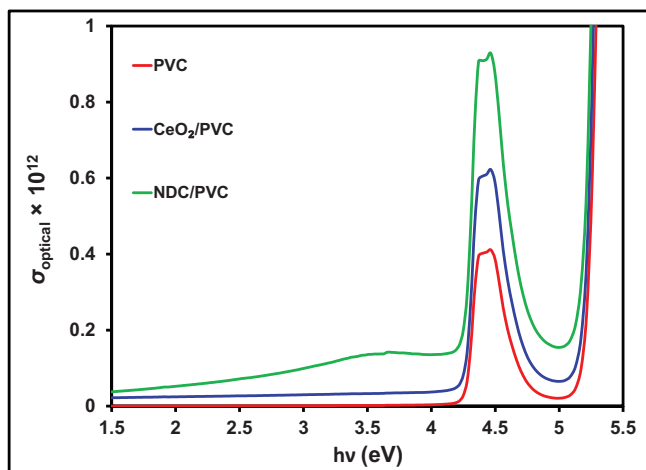


FIGURE 7 | The comparison of the optical conductivity of pure PVC and its NCs.

in Figure 8. The respective micrographs reveal good dispersion of nanofillers while forming a relative homogenous surface of PVC NCs than pure PVC. The decrease in circle edges in NCs as compared to pure PVC shows the successful incorporation of nanofillers into the PVC matrix. Moreover, greater extent of NDC dispersion within the PVC matrix is noticed whereas a relative lower dispersion along with aggregates within the PVC matrix are observable in the respective micrographs. The CeO_2 aggregation formation within PVC matrix has been reduced

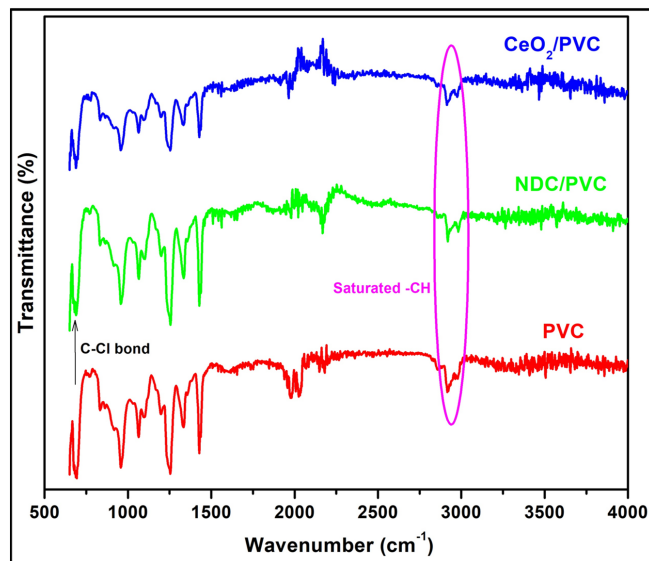


FIGURE 9 | The comparison of FTIR spectra of pure PVC and its NCs.

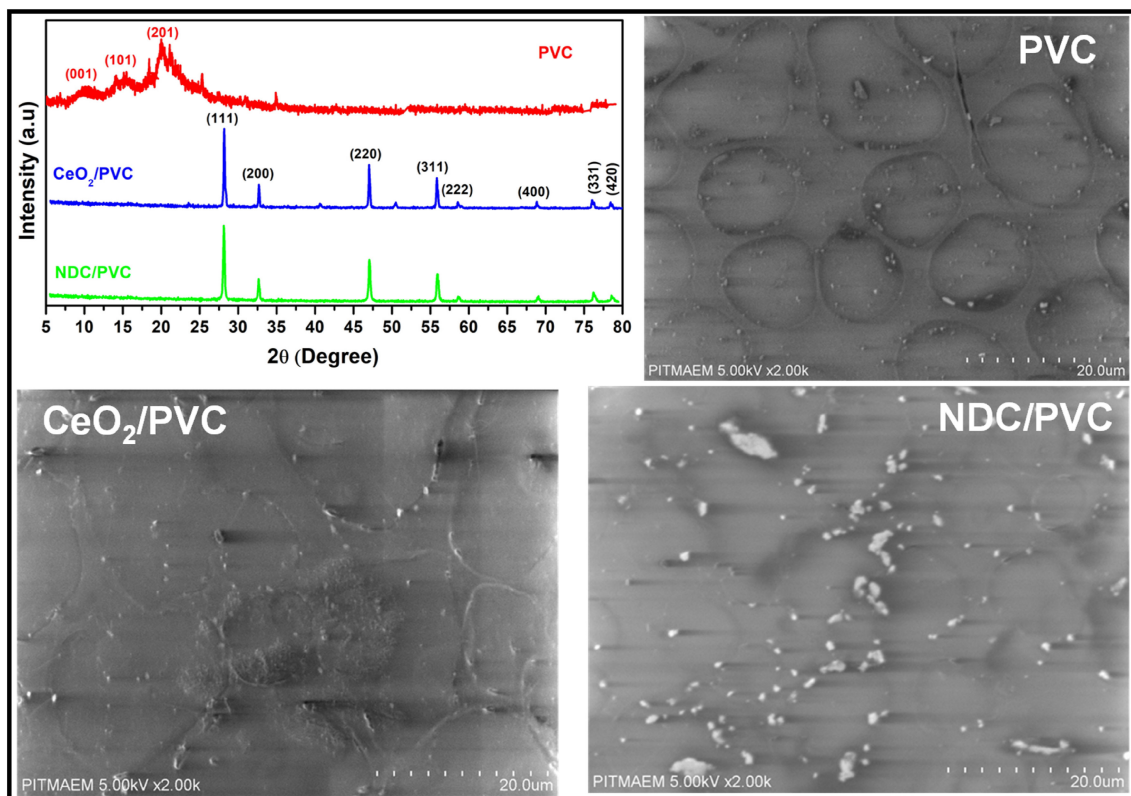


FIGURE 8 | The comparison of XRD patterns and scanning electron micrographs of pure PVC and its NCs.

greatly by incorporating NDC, which represents its greater compatibility with the PVC matrix.

Figure 9 represents the FTIR spectra of pure PVC and its NCs, wherein all the characteristic peaks at $2856\text{--}2979\text{cm}^{-1}$, 1428cm^{-1} , and 1334cm^{-1} about saturated -CH groups of PVC can be seen in NC samples (Abdel-Baset, Elzayat, and Mahrous 2016; Ahmad and Mahmood 2022). Moreover, the appearance of a peak at 693cm^{-1} confirmed the presence of C-Cl stretching due to PVC in NCs (Abdel-Baset, Elzayat, and Mahrous 2016). The display of similar FTIR spectra with slight variation in peak intensities for PVC NCs also reveals the dispersion of nanofillers in the PVC matrix (Ahmed et al. 2023).

The thermal response of PVC and its NCs was investigated using TGA and DSC. The representative thermograms and DSC curves

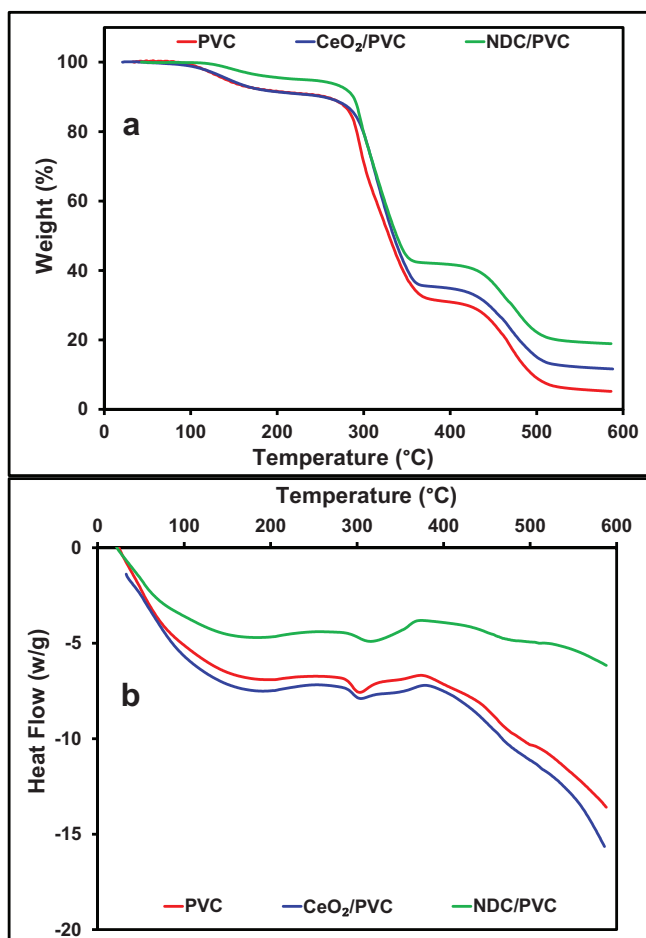


FIGURE 10 | The comparison of (a) TGA and (b) DSC curves of pure PVC and its NCs.

are presented in Figure 10a,b, respectively. Figure 10a shows the three-step degradation of the samples, wherein the 2nd step from $270\text{C}\pm 3^{\circ}\text{C}$ to $420\text{C}\pm 2^{\circ}\text{C}$ is declared as the major weight loss that was occurred due to the dehydrochlorination. This three-step degradation of PVC and its composites is also consistent with previous studies with different nanofillers (Ahmed et al. 2023; Elashmawi et al. 2010). In 3rd step, beyond 400°C , the PVC NCs have lost most of the carbonous polymeric part due to thermal cracking while leaving nanofiller constituents behind. The dehydrochlorination of PVC chains was observed relatively later in NCs in comparison to pure PVC (Figure 10a) which can be attributed to the effective interaction of nanofillers with PVC matrix in order to reduce the release of chlorine which in turn helped in stabilizing the structure of NCs (Faiza et al. 2023). Moreover, another reason in enhancing the thermal stability of the NCs can be the good dispersion of NDC in PVC matrix which helped in effective distribution of thermal stress in the structure. Moreover, the relatively high char yield can be noticed in TGA curve of NDC/PVC in comparison to Pure PVC, which clearly presents the thermal insulating ability of NDC in thermal degradation of PVC (Dastpaki and Khonakdar 2019). Thermal parameters such as T_{10} , T_{50} , and maximum weight loss were estimated from the TG curves and provided in Table 2. DSC curves as shown in Figure 10b, are used to estimate the melting point and glass transition temperature (T_g) of the samples. The melting temperature of PVC was noticed at $\sim 304^{\circ}\text{C}$, whereas the relatively broad melting peaks for CeO_2/PVC and NDC/PVC were observed at $\sim 304^{\circ}\text{C}$ – $\sim 314^{\circ}\text{C}$, respectively. The melting peak broadening in NC as compared to pure PVC indicates concerned interaction between nanofillers and PVC matrix (Mindivan and Göktaş 2020). Moreover, the estimated T_g values (Table 2) revealed a minor variation in NCs in comparison to pure PVC.

4 | Conclusion

NC films of PVC with NDC and CeO_2 were prepared successfully using the solution casting method. The films were characterized by FT-IR, XRD, SEM, TGA/DSC, and UV-visible spectrophotometer and the obtained results were compared with pure PVC film. The optical analysis revealed a decrease in band gap energy of PVC with the addition of NDC from 4.19 to 4.06 eV whereas the increase in other optical constraints such as refractive index, Urbach energy, optical conductivity, dispersion energy, and dielectric constant was observed. The increase in Urbach energy also confirmed the incorporation of nanofillers into the PVC matrix. Furthermore, the presence of nanofillers in PVC was also confirmed due to the existence of their diffraction peaks in XRD patterns of PVC NC films. Thermal analyses revealed higher T_{10} and T_{50} values of NCs in comparison to pure

TABLE 2 | Optical parameters of pure PVC and its NCs with CeO_2 and Ni-doped CeO_2 (NDC).

Thermal Parameter	PVC	CeO_2/PVC	NDC/PVC
T_{10} ($^{\circ}\text{C}$)	256	253	288
T_{50} ($^{\circ}\text{C}$)	329	335	338
Maximum weight loss (%)	95	88	81
Glass transition temperature " T_g " ($^{\circ}\text{C}$)	61	59	62

PVC whereas minor variation in T_g was noticed. A morphology study unveiled the good dispersion of NDC nanofiller in PVC matrix while depleting the circle edges observed in micrographs of pure PVC film.

Author Contributions

Rishum Khan: writing – original draft, formal analysis, data curation. **Muhammad Tariq Qamar:** conceptualization, project administration, resources. **Hina Abid:** methodology, validation, visualization. **Irfan Haider:** writing – review and editing, formal analysis, software, data curation. **Ammar Zidan:** funding acquisition, visualization, validation, formal analysis. **Ali Bahadur:** writing – original draft, project administration, software, formal analysis. **Shahid Iqbal:** conceptualization, supervision, writing – original draft. **Sajid Mahmood:** writing – review and editing, methodology, validation, software. **Mohammed T. Alotaibi:** funding acquisition, writing – review and editing, software, resources. **Toheed Akhter:** investigation, visualization, resources.

Acknowledgments

The authors extend their appreciation to Taif University, Saudi Arabia for supporting this work through project number (TU-DSPP-2024-180).

Conflicts of Interest

The authors declare no conflicts of interest.

Data Availability Statement

The datasets generated during and/or analyzed during the current study are available from the corresponding author upon reasonable request.

References

- Abdel-Baset, T., M. Elzayat, and S. Mahrous. 2016. "Characterization and Optical and Dielectric Properties of Polyvinyl Chloride/Silica NCs Films." *International Journal of Polymeric Science* 2016: 1–13.
- Abdel-Gawad, N. M., A. Z. El Dein, D.-E. A. Mansour, H. M. Ahmed, M. Darwish, and M. Lehtonen. 2017. "Enhancement of Dielectric and Mechanical Properties of Polyvinyl Chloride NCs Using Functionalized TiO₂ Nanoparticles." *IEEE Transactions on Dielectrics and Electrical Insulation* 24, no. 6: 3490–3499.
- Abouhaswa, A., and T. Taha. 2020. "Tailoring the Optical and Dielectric Properties of PVC/CuO NCs." *Polymer Bulletin* 77: 6005–6016.
- Ahmad, N., and T. Mahmood. 2022. "Preparation and Properties of 4-Aminobenzoic Acid-Modified Polyvinyl Chloride/Titanium Dioxide and PVC/TiO₂ Based Nanocomposites Membranes." *Polymers and Polymer Composites* 30: 09673911221099301.
- Ahmed, H. M., Z. M. Abd El-Fattah, N. S. Anad, M. Attallah, and H. H. El-Bahnasawy. 2023. "Thermo-Mechanical and Opto-Electrical Study of Cr-Doped-ZnO-Based Polyvinyl Chloride Nanocomposites." *Journal of Materials Science: Materials in Electronics* 34, no. 2: 113.
- Al-Harbi, L. M., Q. A. Alsulami, M. Farea, and A. Rajeh. 2023. "Tuning Optical, Dielectric, and Electrical Properties of Polyethylene Oxide/Carboxymethyl Cellulose Doped With Mixed Metal Oxide Nanoparticles for Flexible Electronic Devices." *Journal of Molecular Structure* 1272: 134244.
- Alshammari, A. H., K. Alshammari, M. Alshammari, and T. A. M. Taha. 2023. "Structural and Optical Characterization of g-C₃N₄ Nanosheet Integrated PVC/PVP Polymer NCs." *Polymers* 15, no. 4: 871.
- Alshammari, A. H., M. Alshammari, M. Ibrahim, K. Alshammari, and T. A. M. Taha. 2023. "New Hybrid PVC/PVP Polymer Blend Modified

With Er₂O₃ Nanoparticles for Optoelectronic Applications." *Polymers* 15, no. 3: 684.

Asture, A., V. Rawat, C. Srivastava, and D. Vaya. 2023. "Investigation of Properties and Applications of ZnO Polymer NCs." *Polymer Bulletin* 80, no. 4: 3507–3545.

Darwish, M. S., M. H. Mostafa, and L. M. Al-Harbi. 2022. "Polymeric NCs for Environmental and Industrial Applications." *International Journal of Molecular Sciences* 23, no. 3: 1023.

Dastpaki, M., and H. A. Khonakdar. 2019. "Thermal, Thermomechanical, and Morphological Characterization of Poly (Vinyl Chloride) (PVC)/ZnO Nanocomposites: PVC Molecular Weight Effect." *Journal of Vinyl and Additive Technology* 25, no. s2: E63–E71.

Deshmukh, K., S. Khatake, and G. M. Joshi. 2013. "Surface Properties of Graphene Oxide Reinforced Polyvinyl Chloride NCs." *Journal of Polymer Research* 20: 1–11.

Ebinalwaled, A., and A. Thabet. 2016. "Controlling the Optical Constants of PVC Nanocomposite Films for Optoelectronic Applications." *Synthetic Metals* 220: 374–383.

El Sayed, A., S. El-Sayed, W. Morsi, S. Mahrous, and A. Hassen. 2014. "Synthesis, Characterization, Optical, and Dielectric Properties of Polyvinyl Chloride/Cadmium Oxide Nanocomposite Films." *Polymer Composites* 35, no. 9: 1842–1851.

Elashmawi, I., N. Hakeem, L. Marei, and F. Hanna. 2010. "Structure and Performance of ZnO/PVC Nanocomposites." *Physica B: Condensed Matter* 405, no. 19: 4163–4169.

El-Naggar, A., Z. K. Heiba, A. Kamal, O. H. Abd-Elkader, and M. B. Mohamed. 2023. "Impact of ZnS/Mn on the Structure, Optical, and Electric Properties of PVC Polymer." *Polymers* 15, no. 9: 2091.

Faiza, A. Khattak, A. A. Alahmadi, H. Ishida, and N. Ullah. 2023. "Improved PVC/ZnO Nanocomposite Insulation for High Voltage and High Temperature Applications." *Scientific Reports* 13, no. 1: 7235.

Hashmi, S. U. M., M. A. Iqbal, M. Malik, et al. 2022. "Synthesis and Characterization of Polyvinyl Chloride Matrix Composites With Modified Scrap Iron for Advanced Electronic, Photonic, and Optical Systems." *Nanomaterials* 12, no. 18: 3147.

Hemalatha, K., and K. Rukmani. 2016. "Synthesis, Characterization and Optical Properties of Polyvinyl Alcohol-Cerium Oxide Nanocomposite Films." *Royal Society of Chemistry's Advances* 6, no. 78: 74354–74366.

Hu, Z., S. Wang, X. Zhang, et al. 2020. "Simultaneous Enhancements of Ultraviolet-Shielding Properties and Thermal Stability/Photostability of Poly (Vinyl Chloride) via Incorporation of Defect-Rich CeO₂ Nanoparticles." *Industrial & Engineering Chemistry Research* 59, no. 21: 9959–9968.

James, J., A. B. Unni, K. Taleb, et al. 2019. "Surface Engineering of Polystyrene-Cerium Oxide Nanocomposite Thin Films for Refractive Index Enhancement." *Nano-Structures & Nano-Objects* 17: 34–42.

Kassem, S. M., M. Abdel Maksoud, A. M. El Sayed, S. Ebraheem, A. Helal, and Y. Ebaid. 2023. "Optical and Radiation Shielding Properties of PVC/BiVO₄ Nanocomposite." *Scientific Reports* 13, no. 1: 10964.

Kumar, E., P. Selvarajan, and D. Muthuraj. 2012. "Preparation and Characterization of Polyaniline/Cerium Dioxide (CeO₂) Nanocomposite via In Situ Polymerization." *Journal of Materials Science* 47: 7148–7156.

Mallakpour, S., and M. Darvishzadeh. 2018. "Nanocomposite Materials Based on Poly (Vinyl Chloride) and Bovine Serum Albumin Modified ZnO Through Ultrasonic Irradiation as a Green Technique: Optical, Thermal, Mechanical and Morphological Properties." *Ultrasonics Sonochemistry* 41: 85–99.

Mallakpour, S., and E. Shafiee. 2017. "The Synthesis of Poly (Vinyl Chloride) Nanocomposite Films Containing ZrO₂ Nanoparticles Modified With Vitamin B1 With the Aim of Improving the Mechanical,

Thermal and Optical Properties.” *Designed Monomers and Polymers* 20, no. 1: 378–388.

Mansour, D.-E. A., N. M. Abdel-Gawad, A. Z. El Dein, H. M. Ahmed, M. M. Darwish, and M. Lehtonen. 2020. “Recent Advances in Polymer NCs Based on Polyethylene and Polyvinylchloride for Power Cables.” *Materials* 14, no. 1: 66.

Mindivan, F., and M. Göktaş. 2020. “Preparation of New PVC Composite Using Green Reduced Graphene Oxide and Its Effects in Thermal and Mechanical Properties.” *Polymer Bulletin* 77, no. 4: 1929–1949.

Mishra, G., and M. Mukhopadhyay. 2021. “Well Dispersed CeO₂@HNTs Nanofiller in the Poly (Vinyl Chloride) Membrane Matrix and Enhanced Its Antifouling Properties and Rejection Performance.” *Journal of Environmental Chemical Engineering* 9, no. 1: 104734.

Patidar, D., and N. S. Saxena. 2013. “Influence of CdS Nano Additives on the Thermal Conductivity of Poly (Vinyl Chloride)/CdS NCs.” *Advances in Nanoparticles* 2, no. 1: 11–15.

Qamar, M. T., S. Iqbal, A. Bilal, et al. 2023. “Transition Metal Doped CeO₂ for Photocatalytic Removal of 2-Chlorophenol in the Exposure of Indoor White Light.” *Frontiers in Chemistry* 11: 1126171.

Rahman, M., M. A. Hoque, G. Rahman, M. Gafur, R. A. Khan, and M. K. Hossain. 2019. “Study on the Mechanical, Electrical and Optical Properties of Metal-Oxide Nanoparticles Dispersed Unsaturated Polyester Resin NCs.” *Results in Physics* 13: 102264.

Romero-Fierro, D., M. Bustamante-Torres, F. Bravo-Plascencia, H. Magaña, and E. Bucio. 2022. “Polymer-Magnetic Semiconductor NCs for Industrial Electronic Applications.” *Polymers* 14, no. 12: 2467.

Safdari, S. M., S. Malekie, S. Kashian, and M. Akbari. 2022. “Introducing a Novel Beta-Ray Sensor Based on Polycarbonate/Bismuth Oxide Nanocomposite.” *Scientific Reports* 12, no. 1: 1–10.

Taha, T., and A. Azab. 2019. “Thermal, Optical, and Dielectric Investigations of PVC/La_{0.95}Bi_{0.05}FeO₃ NCs.” *Journal of Molecular Structure* 1178: 39–44.

Taha, T., Z. Ismail, and M. Elhawary. 2018. “Structural, Optical and Thermal Characterization of PVC/SnO₂ NCs.” *Applied Physics A* 124: 1–13.

Tamayo-Vegas, S., A. Muhsan, C. Liu, M. Tarfaoui, and K. Lafdi. 2022. “The Effect of Agglomeration on the Electrical and Mechanical Properties of Polymer Matrix NCs Reinforced With Carbon Nanotubes.” *Polymers* 14, no. 9: 1842.

Zhang, C., H. Khorshidi, E. Najafi, and M. Ghasemi. 2023. “Fresh, Mechanical and Microstructural Properties of Alkali-Activated Composites Incorporating Nanomaterials: A Comprehensive Review.” *Journal of Cleaner Production* 384: 135390.

Zhang, Y., Z. Huang, H. Wang, and J. Li. 2023. “Regulation of the Interface Compatibility of the 3D-Printing Interpenetration Networks Toward Reduced Structure Anisotropy and Enhanced Performances.” *ACS Applied Materials & Interfaces* 15, no. 27: 32984–32992.